

Article

Modular Spiral Heat Exchanger Thermal Modelling

Bystrík Červenka, Michal Holubčík * , Juraj Drga and Milan Malcho 

Department of Power Engineering, Faculty of Mechanical Engineering, University of Žilina, Univerzitná 1, 010 26 Žilina, Slovakia; cervenka2@stud.uniza.sk (B.Č.); juraj.drga@fstroj.uniza.sk (J.D.); milan.malcho@fstroj.uniza.sk (M.M.)

* Correspondence: michal.holubcik@fstroj.uniza.sk

Abstract: Spiral plate heat exchangers (SPHEs) are used in industrial applications due to their enhanced thermal performance and tolerance to a soiled stream. The coupling of several SPHEs in series might further improve performance in terms of the effectiveness parameter. In the present study, a compact connection of several SPHE modules is proposed and investigated. For this purpose, a numerical model for the prediction of the effectiveness parameter of a modular SPHE was developed. The model predicted a 2.9% increase in the maximal effectiveness for a two-module SPHE in comparison to a conventional single module SPHE. The temperature profiles of particular streams within the two-module SPHE were predicted. The improved thermal performance and compactness of the modular SPHE configuration observed is advantageous for space-constrained applications.

Keywords: spiral plate; heat exchanger; modular configuration; thermal model; effectiveness



Citation: Červenka, B.; Holubčík, M.; Drga, J.; Malcho, M. Modular Spiral Heat Exchanger Thermal Modelling. *Appl. Sci.* **2022**, *12*, 5805. <https://doi.org/10.3390/app12125805>

Academic Editors: Fabio Polonara, Vítor António Ferreira da Costa, Sandro Nizetic and Alice Mugnini

Received: 18 May 2022

Accepted: 4 June 2022

Published: 7 June 2022

Publisher's Note: MDPI stays neutral with regard to jurisdictional claims in published maps and institutional affiliations.



Copyright: © 2022 by the authors. Licensee MDPI, Basel, Switzerland. This article is an open access article distributed under the terms and conditions of the Creative Commons Attribution (CC BY) license (<https://creativecommons.org/licenses/by/4.0/>).

1. Introduction

The spiral type of heat exchanger is applied in many types of process industry due to a number of positive features of its design. Improved compactness of the exchanger arises from an enhanced heat transfer coefficient in curved channels. Applications in the chemical process industry are enabled by the single channel design of the SPHE and its resistance to fouling. The low thermal leakage to the ambient environment and the ability of SPHEs to absorb thermal dilatation are advantageous for high temperature applications.

Minton [1] provided a comprehensive set of correlation formulae for the heat transfer coefficient and the pressure drop for various SPHE configurations, which are potentially useful in the preliminary stages of heat exchanger design. Studies by Picón-Núñez [2] and Shirazi et al. [3] focused on SPHE design utilizing available pressure heads for particular applications.

Bidabadi et al. [4] made use of developed thermal correlations for the dedicated optimization of SPHE performance and reduction in costs.

Bes and Roetzel [5–7] used Laplace transformation and Hermite polynomials to provide a solution for the SPHE energy balance equation and prediction of the effectiveness parameter. Bounopane, Troupe [8], Strenger et al. [9] and Nguyen and San [10] applied numerical integration and numerical solution tools on the resulting system of differential equations for SPHE performance prediction. Computer algebra systems were used in studies by Target et al. [11] and Burmeister [12] to determine closed formulae, which could offer theoretical tools for the study of the heat transfer performance of SPHEs. Djordjević et al. [13] built a 3D numerical model and used a commercial CFD solver for the investigation of the wall heat transfer coefficient.

The present study proposes a compact, serial thermal coupling of several SPHEs. This configuration is designed to improve the thermal performance of the resulting modular SPHE design. A numerical model for the modular SPHE was developed to predict the heat transfer effectiveness parameter.

Although similar numerical models have been presented in other studies, to the author’s knowledge, no application of the modular SPHE configuration has been presented to date.

Moreover, there is a subtle difference in the mathematical formulation that is used in the present model compared to those provided in previous reports. The main aim of the study was to investigate the heat transfer effectiveness parameter as a function of the number of spiral turns and the stream temperature profiles in a two-module SPHE.

The modular design proposed is suitable for constrained space applications and production processes in which there are restrictions, e.g., the injection of high conductivity plastic materials.

2. Materials and Methods

2.1. Geometry Model

The usual SPHE configuration consists of one layer, here referred to as a module, of double spiral walls, which create two separate channels for the hot and cold streams. The hot stream enters the central core of the exchanger and the cold stream is introduced at the periphery of the studied SPHE (Figure 1a). This stream configuration provides a counter flow of streams.

The other SPHE configuration investigated in the study is a two-module SPHE. It is composed of two one-module SPHEs connected in series with a counterflow stream configuration (Figure 1b). The two modules of the exchanger are connected by a shared end wall with openings at the peripheries of the hot and cold channels, respectively, which allows for their shortest possible serial connection.

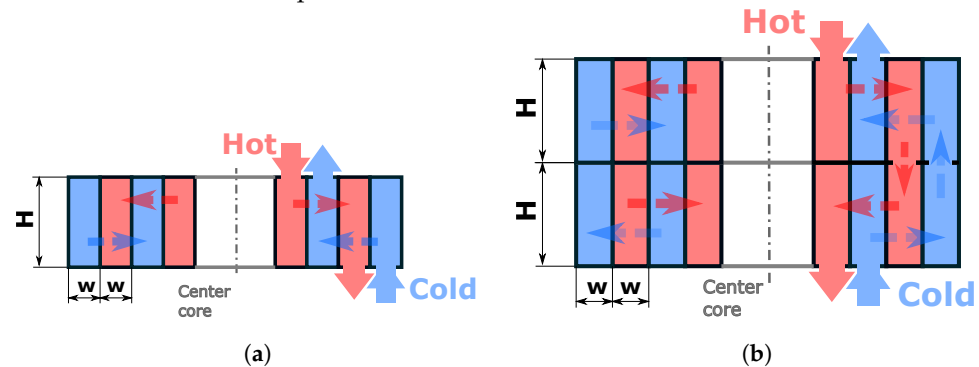


Figure 1. Schematic configurations of SPHE: (a) Single module SPHE. (b) Two-module SPHE.

The heat exchanging spiral walls are configured such that the stream channels start and end at the same angle, thus producing the same number of turns, as shown in Figure 2.

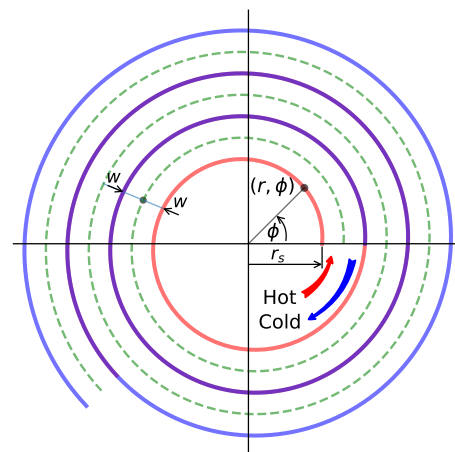


Figure 2. SPHE channel geometry configuration and depicted model parameters.

The wall geometry of the SPHE investigated is composed of an Archimedean spiral, defined by equation

$$r = a\phi + r_s, \tag{1}$$

where ϕ —the angular coordinate, r_s —the starting radius of a spiral (at $\phi = 0$), and a —the parameter of the Archimedean spiral defined by $a = w / \pi$, with w being the width of the hot and cold channels, respectively.

The differential length of the spiral arc heat transfer surface area is expressed by

$$dl = \sqrt{r^2 + \left(\frac{dr}{d\phi}\right)^2} d\phi = \sqrt{r^2 + a^2} d\phi. \tag{2}$$

Utilizing Equation (1), introducing the turn number coordinate from the spiral start $\phi = \frac{\phi}{2\pi}$, relative to the spiral starting radius parameter $z_s = \frac{r_s}{2\pi a}$, the differential arc length of the spiral, starting at a radius of r_s , is represented by

$$dl = 4\pi^2 a \sqrt{(\phi + z_s)^2 + \frac{1}{4\pi^2}} d\phi. \tag{3}$$

The numerical model developed here was compared to the results published for the geometry by Strenger et al. [9], as shown in Figure 3a. The results for a two-module (2M) SPHE, with an equivalent surface area, are presented. The equivalent 2M SPHE is shown in Figure 3b in comparison to the SPHE geometry provided by Strenger et al. [9].

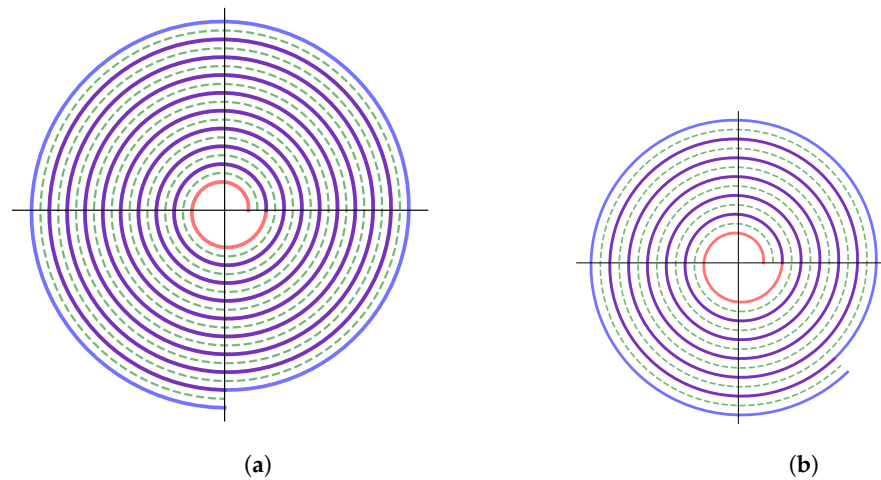


Figure 3. Investigated SPHE geometry configurations: (a) Configuration investigated by Strenger et al. [9], $N_t = 8.75$. (b) Two-module SPHE geometry with equivalent area to the SPHE of Strenger et al. [9], $N_t = 5.6$.

2.2. Mathematical Model

The thermal model of the SPHE is based on the following assumptions:

- steady state performance of the SPHE
- no heat loss to the ambient environment through the inner and outer surfaces and the exchanger end walls
- neglected axial conduction in the SPHE
- the middle surface of the spiral walls is considered as a heat transfer area between the hot and cold channels
- neglected variation in the stream’s thermal properties for both streams.

The application of the energy balance on the SPHE control volume, defined by the angular section $d\phi$, and the application of the assumption leads to:

$$\begin{aligned} C_H dT_H &= U_{in} dA_{H,in} (T_{C,in} - T_H) + U_{ou} dA_{H,ou} (T_{C,ou} - T_H), \\ -C_C dT_C &= U_{in} dA_{C,in} (T_{H,in} - T_C) + U_{ou} dA_{C,ou} (T_{H,ou} - T_C), \end{aligned} \tag{4}$$

where: $T_{H,C}$ —the hot and cold stream temperatures, respectively, $C_{H,C}$ —the thermal capacitance rate of the hot and cold streams, respectively, $U_{in,ou}$ —the overall heat transfer coefficient between the evaluated channel and the inner and outer channels, respectively, $dA_{H,C,in,ou}$ —the differential heat transfer middle spiral surface towards the neighboring inner and outer walls of the hot and cold channels, respectively, and $T_{H,C,in,ou}$ —the temperature in the neighboring inner and outer hot and cold streams, respectively.

Making use of Equation (3) for differential area evaluation and introducing the following non-dimensional parameters:

$$u_{in} = \frac{U_{in}}{U}, \quad u_{ou} = \frac{U_{ou}}{U}, \quad C_H^* = \frac{C_H}{C_{min}}, \quad t_H = \frac{(T_H - T_{C,1})}{(T_{H,1} - T_{C,1})},$$

where: U —the SPHE average overall heat transfer coefficient, $T_{C,H,1}$ —the inlet temperature of the hot and cold streams, respectively, C_{min} —the minimal thermal capacitance rate, Equation (5) are obtained for the hot and cold streams at an intermediate part of the SPHE

$$\begin{aligned} \frac{dt_H}{d\varphi} &= NTU \frac{4\pi^2 a}{C_H^* L_t} \left[u_{in} \sqrt{\left(\varphi + z_{H,s} - \frac{1}{4}\right)^2 + \frac{1}{4\pi^2} (t_{C,in} - t_H)} + u_{ou} \sqrt{\left(\varphi + z_{H,s} + \frac{1}{4}\right)^2 + \frac{1}{4\pi^2} (t_{C,ou} - t_H)} \right], \\ \frac{dt_C}{d\varphi} &= - NTU \frac{4\pi^2 a}{C_C^* L_t} \left[u_{in} \sqrt{\left(\varphi + z_{C,s} - \frac{1}{4}\right)^2 + \frac{1}{4\pi^2} (t_{H,in} - t_C)} + u_{ou} \sqrt{\left(\varphi + z_{C,s} + \frac{1}{4}\right)^2 + \frac{1}{4\pi^2} (t_{H,ou} - t_C)} \right], \end{aligned} \tag{5}$$

where in Equation (5): NTU —the SPHE total number of transfer units, and L_t —the total length of the double spiral.

The Equation (5) are valid for inner and outer turns of the SPHE, without a neighboring channel for heat exchange, with $u_{in,ou} = 0$ for the respective spiral turns.

The boundary conditions for Equation (5) are: $T_H(\varphi = 0) = 1$, and $T_C(\varphi = \varphi_e) = 0$, where φ_e is the angular coordinate of the cold channel inlet.

The assessment of the two-module SPHE is based on a performance prediction for the coupled heat exchangers connected in series in a counterflow configuration with $C_r = 1$. The relation between the total and the individual module effectiveness of a two-module SPHE stated in Roetzel, Spang [14] is

$$\frac{\epsilon_t}{1 - \epsilon_t} = \frac{n_m \epsilon}{1 - \epsilon'} \tag{6}$$

where: ϵ_t —the total effectiveness of a two-module SHE, ϵ —the individual effectiveness of a one-module SPHE, and n_m —the number of modules.

2.3. Numerical Model

A finite difference method with an upwind scheme was used to discretize Equation (5) in the present study. The resulting system of algebraic equations were solved using the Gauss–Seidel relaxation technique. The convergence criteria are given by a reduction in the non-dimensional temperature change between the subsequent iterations by less than 1×10^{-7} .

A mesh independence study showed no significant change in the results for a density of 160 nodes per half turn of the spiral channel.

The first-order accuracy of the implemented scheme was compensated by an increased mesh resolution. The chosen numerical scheme proved to be robust and converged to a steady solution in a reasonable time, independent of the mesh density and NTU values. The advantages of the implemented method are its implementation efficiency and its general applicability.

3. Results and Discussion

3.1. One-Module SPHE

The variation in the SPHE effectiveness, as predicted by the present model, on NTU was compared to results published for other studies, as shown in Figure 4. The SPHE geometry used in the work of Strenger et al. [9], with $Nt = 8.75$, was used for comparison.

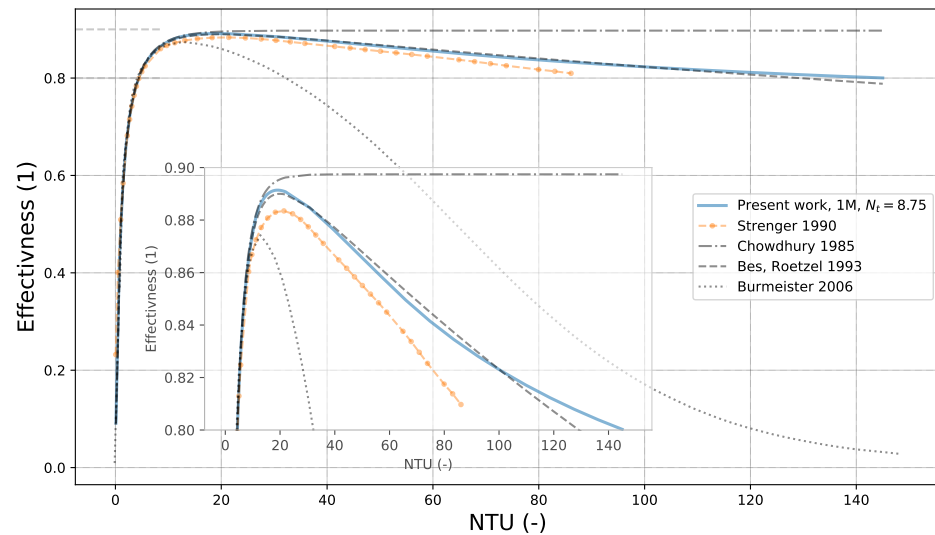


Figure 4. Prediction of the effectiveness parameter for a one-module (1M) SPHE in comparison to results from the literature.

The presented effectiveness variation was in good agreement (a difference less than 0.6%) with results obtained by the model of Bes and Roetzel [5] across the whole range of NTU values studied. There was visibly lower effectiveness observed in this investigation compared to the study of Strenger et al. [9], probably due to a difference in the geometry configuration.

It should be noted that there was a difference in π in the angular offset of the stream inlets and outlets in the two geometries. However, a noticeable shift in both the optimal NTU value and the maximal effectiveness was evident by comparison to the model of Burmeister [12].

The maximal value of effectiveness, as well as the optimal NTU value, were predicted very closely in the present investigation and using the model of Bes, Roetzel [5]. There was, however, change in the slope of the effectiveness curve between the two models in the upper range of the studied NTU. There was another local minimum in the $NTU - \epsilon$ curve, especially for small numbers of N_t . It is inferred that the effectiveness curve asymptotically approaches a value of 1 at increased NTU values, as is obvious for smaller Nt values in Figure 5. The model shows that a two-module SPHE with $N_t = 2.375$ shifts the maximum effectiveness, as well as the NTU_o , to a higher level compared to a one-module SPHE with $N_t = 3.625$, having the same total area.

This behavior was due to the increasing effect of the purely counterflow heat exchange manifest in the central core and the periphery of the SPHE model investigated. The same explanation for the behavior was assumed by Burmeister [12].

The present model was able to represent the features for maximal effectiveness for finite, optimal values of NTU, characteristic of plate-type heat exchangers, including SPHEs. These features have been overlooked by SPHE designers for a long time, with Strenger et al. [9] being among the first researchers to notice them. However, a correlation-based model proposed by Chowdhury et al. [15] and Martin [16] was not able to capture the behavior. The effectiveness parameter continuously increased with increasing NTU in their model.

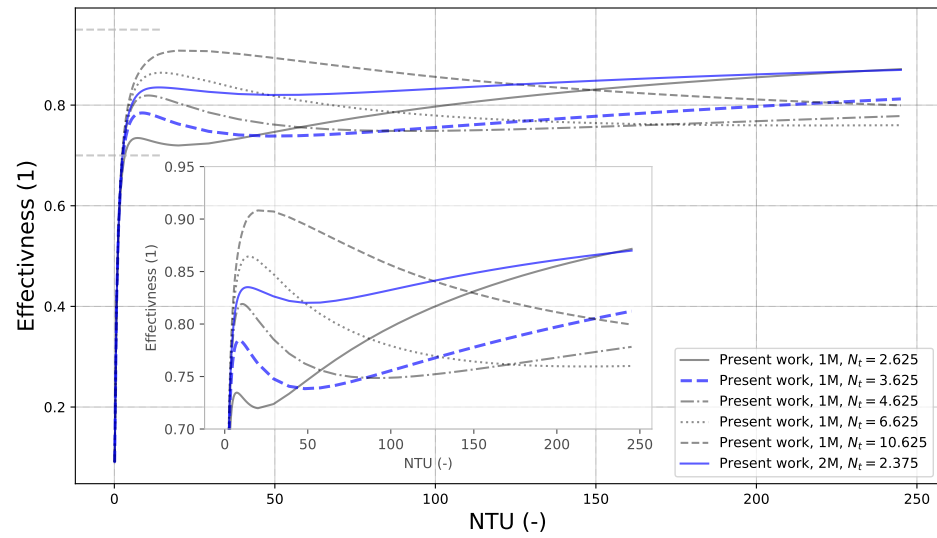


Figure 5. Effect of N_t on predicted effectiveness parameter for one- and two-module SPHEs. 2M, $N_t = 2.375$ is equivalent to 1M, $N_t = 3.625$.

The maximal effectiveness of an SPHE is linked to the relative temperature level of the cold stream and the temperature in the two hot streams surrounding the cold stream. The temperature variation for the proposed model with positions along the channel are given by the turn number, as presented in Figure 6 for three values of NTU. The predicted variation was in agreement with the explanation provided by Strenger et al. [9].

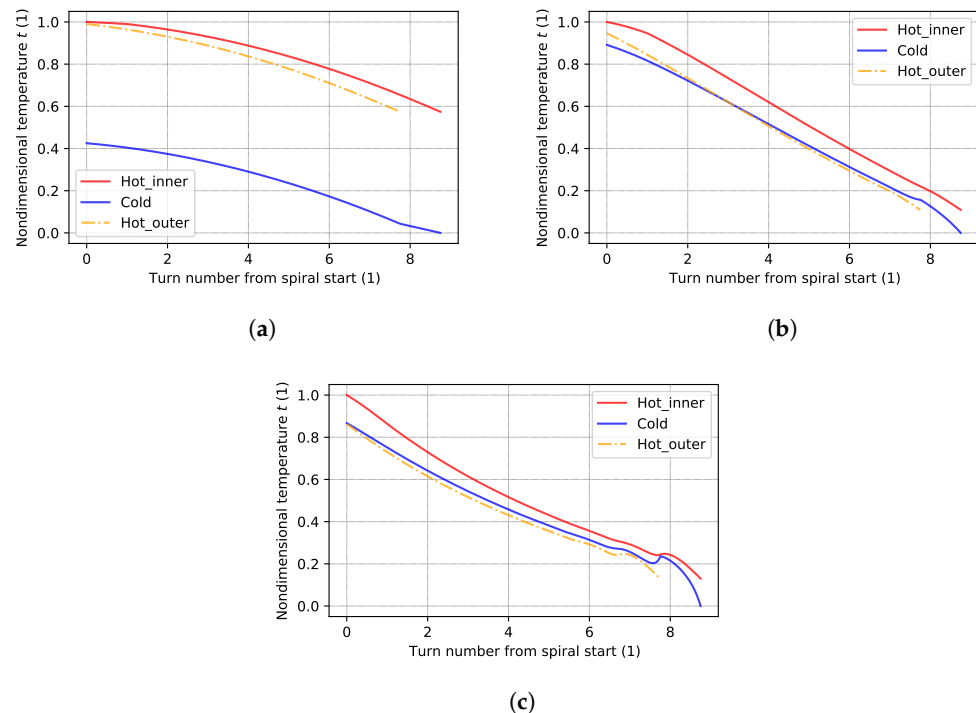


Figure 6. Predicted temperature profile in one-module SPHE with geometry from Strenger et al. [9]. (a) Low NTU. (b) Optimal NTU. (c) High NTU.

3.2. Two Module SPHE

The proposed model was applied to a two-module SPHE configuration, as shown in Figure 1b, with an equivalent total heat transfer area to that of Strenger et al. [9]. The computed effectiveness parameter variation was compared to a one-module and ideal counter-flow heat exchanger, as shown in Figure 7.

The present model predicted increased effectiveness of a two-module SPHE compared to a one-module SPHE across the whole NTU range. The results for a two-module SPHE indicated an increase in the maximal effectiveness of 2.9%. The optimal NTU value for a two-module SPHE is shifted to $NTU_{0,2M} = 26.5$ in comparison to an equivalent to a one-module SPHE $NTU_{0,1M} = 18.5$.

The predicted individual effectiveness parameter of a one-spiral module is in agreement with the prediction based on the Bes and Roetzel [5] model and the relation between the total and individual effectiveness parameters given by Equation (6).

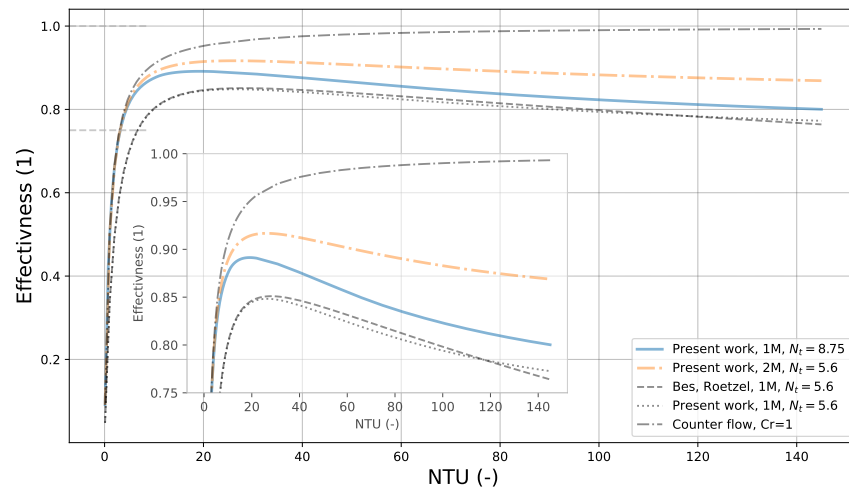


Figure 7. Comparison of the predicted effectiveness parameter for one- and two-module SPHE. 2M, $N_t = 5.6$ is equivalent to 1M, $N_t = 8.75$ SPHE.

The variation in the cold stream temperature and the temperature in the inner and outer neighboring hot streams is shown in Figure 8 for the three distinctive NTU values. There was a temperature cross between the cold stream and its inner hot stream in the first SPHE module, as shown in Figure 8b. The temperature cross of the same cold stream was predicted with its outer hot stream in the second SPHE module.

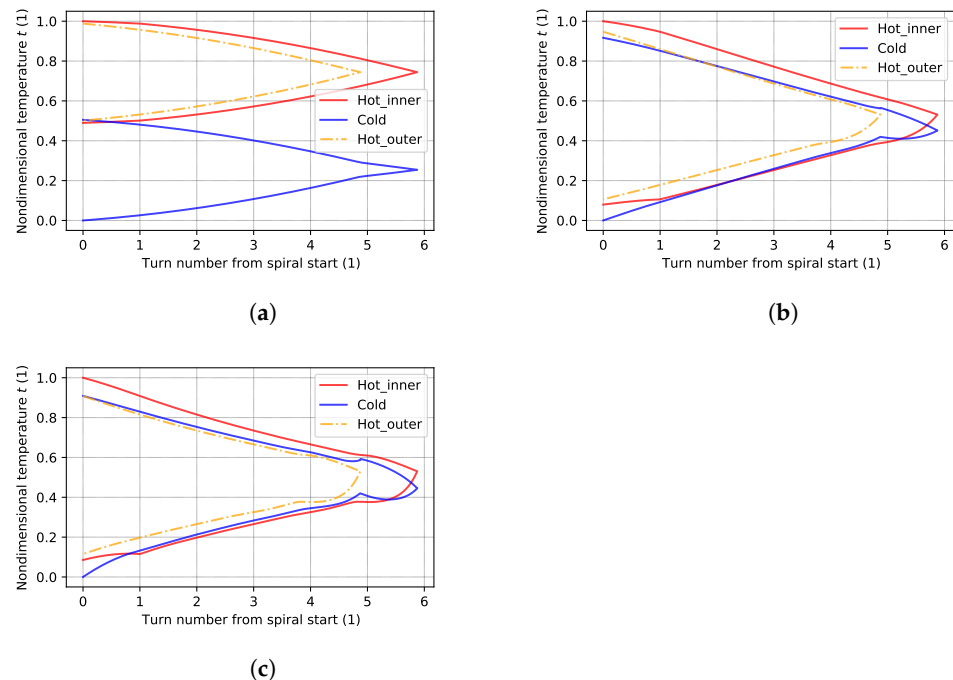


Figure 8. Predicted temperature profile in two-module SPHE with equivalent geometry to Strenger et al. [9]. (a) Low NTU. (b) Optimal NTU. (c) High NTU.

4. Conclusions

The predicted SPHE performance parameters for the proposed model agreed well with the theoretical model, as well as with numerical predictions from previous studies. The model was able to predict the features of local maximal effectiveness, which are characteristic of SPHEs.

The model was extended and applied to a two-module SPHE and predicted superior performance compared to a one-module SPHE with the same total heat transfer area. The maximal effectiveness level was predicted to be higher by 2.9% compared to the equivalent one-module SPHE. The increased relative portion of the heat exchanger area, experiencing pure counterflow heat transfer at the central core and mainly on the periphery of the SPHE, was responsible for the improved performance.

The prediction showed decreased optimal values of NTU with decreased number of turns for both one- and two-module SPHEs. There was a predicted exchange between the temperature levels in the cold and hot streams for the first and second modules of the two-module SPHE.

The improved effectiveness parameters of the two-module SPHE could further enhance the compactness of the SPHE.

Author Contributions: B.Č., conceptualization, investigation, software, validation, writing—original draft; M.H., methodology, formal analysis, resources, writing—review and editing, funding, acquisition; J.D., data curation, visualization; M.M., formal analysis, methodology, writing—review and editing. All authors have read and agreed to the published version of the manuscript.

Funding: This research was funded within the framework of projects: VEGA 1/0233/19 Structural modification of a burner for the combustion of solid fuels in small heat sources; VEGA 1/0479/19 Effect of combustion condition on production of solid polluting particles in small heat sources; and, KEGA 032ŽU-4/2022 Implementation of knowledge about modern ways of reducing environmental burden in the energy use of solid fuels and waste into the pedagogical process.

Conflicts of Interest: The funders had no role in the design of the study; in the collection, analyses, or interpretation of data; in the writing of the manuscript, or in the decision to publish the results. The authors declare no conflict of interest.

Abbreviations

The following abbreviations are used in this manuscript:

CFD	computational fluid dynamics
SPHE	spiral plate heat exchanger
1M	one module
2M	two module

References

1. Minton, P. Designing Spiral-Plate Exchangers. *Chem. Eng. Prog.* **1970**, *77*, 103–112.
2. Picón-Núñez, M.; Canizalez-Dávalos, L.; Martínez-Rodríguez, G.; Polley, G.T. Shortcut Design Approach for Spiral Heat Exchangers. *Food Bioprod. Process.* **2007**, *58*, 322–327. [[CrossRef](#)]
3. Sabouri Shirazi, A.H.; Jafari Nasr, M.R.; Ghodrat, M. Effects of Temperature Differences in Optimization of Spiral Plate Heat Exchangers. *Process Integr. Optim. Sustain.* **2020**, *4*, 391–408. [[CrossRef](#)]
4. Bidabadi, M.; Sadaghiani, A.; Azad, V. Spiral heat exchanger optimization using genetic algorithm. *Sci. Iran. B* **2013**, *20*, 1445–1454.
5. Bes, T.; Roetzel, W. Thermal Theory of the Spiral Heat Exchanger. *Int. J. Heat Mass Transf.* **1993**, *36*, 765–773. [[CrossRef](#)]
6. Bes, T.; Roetzel, W. Approximate Theory of Spiral Heat Exchanger. In Proceedings of the EURO THERM Seminar No. 18, Hamburg, Germany, 27 February–1 March 1991; Springer: Berlin/Heidelberg, Germany, 1991; pp. 223–232.
7. Bes, T. Eine Methode der thermische Berechnung von Gegen- und Gleichstrom-Spiralwärmeaustauschern. *Wärme- und Stoffübertragung* **1987**, *21*, 301–309. [[CrossRef](#)]
8. Buonopane, R.; Troupe, R. Analytical and Experimental Heat Transfer Studies in a Spiral Plate Heat Exchanger. In Proceedings of the IV International Heat Transfer Conference, Paris, France, 31 August–5 September 1970; Volume I, pp. 1–11.
9. Strenger, M.; Churchill, S.; Retallick, W. Operational Characteristics of a Double-Spiral Heat Exchanger for the Catalytic Incineration of Contaminated Air. *Int. Eng. Chem. Res.* **1990**, *29*, 1977–1984. [[CrossRef](#)]

10. Nguyen, D.K.; San, J.Y. Heat Transfer and Exergy Analysis of a Spiral Heat Exchanger. *Heat Transf. Eng.* **2016**, *37*, 1013–1026. [[CrossRef](#)]
11. Targett, M.J.; Retallick, W.B.; Churchill, S.W. Solutions in Closed Form for a Double-Spiral Heat Exchanger. *Ind. Eng. Chem. Res.* **1992**, *31*, 658–669. [[CrossRef](#)]
12. Burmeister, L. Effectiveness of a Spiral-Plate Heat Exchanger with Equal Capacitance Rates. *J. Heat Transfer* **2006**, *128*, 295–301. [[CrossRef](#)]
13. Djordjević, M.; Stefanovic, V.; Vukić, M.; Mančić, M. Numerical investigation on the convective heat transfer in a spiral coil with radiant heating. *Therm. Sci.* **2016**, *20*, 1215–1226. [[CrossRef](#)]
14. Roetzel, W.; Spang, B. 11. Auflage; chapter Berechnung von Wärmeübertragern. In *VDI-Wärmeatlas*; Springer: Berlin/Heidelberg, Germany, 2013; pp. 39–74.
15. Chowdhury, K.; Linkmeyer, H.; Bassiouny, M.; Martin, H. Analytical Studies on the Temperature Distribution in Spiral Plate Heat Exchangers: Straightforward Design Formulae for Efficiency and Mean Temperature Difference. *Chem. Eng. Process.* **1985**, *19*, 183–190. [[CrossRef](#)]
16. Martin, H. *Heat Exchangers*; Hemisphere Publishing Co.: Washington, DC, USA; Philadelphia, PA, USA; London, UK, 1992; pp. 142–149.